

A RAPID METHOD FOR DISTINGUISHING VACANCY
AND INTERSTITIAL LOOPS IN ION IMPLANTED CRYSTALS

K. Seshan, W. L. Bell, and J. Washburn

August 1972

AEC Contract No. W-7405-eng-48

For Reference

Not to be taken from this room



DISCLAIMER

This document was prepared as an account of work sponsored by the United States Government. While this document is believed to contain correct information, neither the United States Government nor any agency thereof, nor the Regents of the University of California, nor any of their employees, makes any warranty, express or implied, or assumes any legal responsibility for the accuracy, completeness, or usefulness of any information, apparatus, product, or process disclosed, or represents that its use would not infringe privately owned rights. Reference herein to any specific commercial product, process, or service by its trade name, trademark, manufacturer, or otherwise, does not necessarily constitute or imply its endorsement, recommendation, or favoring by the United States Government or any agency thereof, or the Regents of the University of California. The views and opinions of authors expressed herein do not necessarily state or reflect those of the United States Government or any agency thereof or the Regents of the University of California.

A RAPID METHOD FOR DISTINGUISHING VACANCY AND INTERSTITIAL
LOOPS IN ION IMPLANTED CRYSTALS

K. Seshan, W. L. Bell* and J. Washburn

Inorganic Materials Research Division, Lawrence Berkeley Laboratory and
Department of Materials Science and Engineering, College of Engineering;
University of California, Berkeley, California

ABSTRACT

Loop nature (interstitial or vacancy) may be rapidly and consistently determined using dark-field images at small deviations from the Bragg position. Contrast analysis provides the inclination of the loop planes, given some planar or linear defect of known orientation in the field of view. Image flipping from "outside" to "inside" contrast may then be used to determine loop character.

Plane inclinations may also be determined by the usual more involved large angle tilt experiment combined with Kikuchi analysis. It is shown that the above two methods give the same result. The contrast method is more rapid, not requiring accurate orientation determination or a high angle goniometer tilt stage. Examples are presented for loops in annealed phosphorous ion implanted silicon. The loops are shown to be predominantly interstitial in accord with the findings of other workers.

* Present address: General Electric Company, Vallecitos Atomic Laboratory, Pleasanton, CA 94566

INTRODUCTION

Bell and Thomas^{1,2} and Thomas³ have demonstrated that contrast analysis of dark-field images at non-Bragg positions can determine the inclination of a plane or direction if the field of view contains a planar or linear defect of known crystallographic orientation which extends at an oblique angle from top to bottom of the foil. Dark-field micrographs with s (the deviation parameter) positive show good contrast for defects near the bottom of the foil. Those with s -negative show good contrast for defects near the top of the foil. In the case of annealed phosphorous ion implanted silicon studied here linear rod-like defects lying along $\langle 110 \rangle$ directions and inclined to the (111) surface of the foil were used in the contrast analysis. The dark-field micrographs determine which end of the rod lies near the top and which near the bottom of the foil. Once two of the six $\langle 110 \rangle$ directions are fixed (the operating reflection and the direction of the inclined rod) the inclination of all planes and directions are found. Given the loop habit-plane, the inclination of the loop with respect to the foil surface for a given loop is known. Loop sense (vacancy or interstitial) can then be determined for a large number of loops.

The inclination of a linear or planar defect can also be determined by the conventional large angle rotation method. The specimen is rotated through about 12° and stereographic and Kikuchi analysis are used to determine plane inclinations.

Some authors⁴ have questioned the validity of associating a habit plane and Burger's vector with the line of no contrast of a double arc image of a dislocation loop. For extremely small loops (less than 100\AA),

visible only by strain contrast, the criticism is justified. However, for dislocation loops produced during the annealing of ion damage in silicon it is shown here that consistent interpretation using the double-arc model is possible at least for loops larger than 500Å.

EXPERIMENTAL

Samples of p-type silicon (5Ω-cm, Boron doped) were implanted to a dose of 2×10^{14} phosphorous ions/cm² at 100 kV. The resulting damage was annealed at 800°C for half an hour. Samples were chemically thinned and examined in a Siemens 1A electron microscope at 100 kV. The annealing treatment resulted in large numbers of small dislocation loops with Burgers vector $a/2 \langle 110 \rangle$ type and linear defects that lay along $\langle 110 \rangle$ directions.^{5,6}

CONTRAST EXPERIMENTS

The Bell and Thomas criterion utilizes the fact that for the s-negative condition defects near the top of the foil are in good contrast and for the s-positive condition, defects near the bottom of the foil are in good contrast. This criterion can be applied to the dark-field micrographs of Figs. 1 and 2. The field of view contains a rod defect at X which is known to lie along $\langle 110 \rangle$ and extends from near the top surface to near the bottom surface of the foil.

In Fig. 1 (dark-field, s-negative) the top of the foil is expected to be in good contrast. Therefore, the end of the inclined rod marked X is near the top of the foil. On the other hand, in Fig. 2 (dark-field, s-positive) the end of the rod away from X is seen in good oscillating contrast. This end must then be near the bottom of the foil.

Since two $\langle 110 \rangle$ directions (the operating reflection $\bar{g}[1\bar{1}0]$

and the direction of inclination of the rod X) are now known, all other crystallographic planes and directions can be defined. The resulting inclination of the (111) planes are drawn in Fig. 3.

LOOP ANALYSIS

Since the inclination of the fault plane, the operating reflection \bar{g} and the deviation parameter is known, loop sense may be determined by studying the image position with respect to the true defect position. Two of the six possible loop variants are marked α and β . One variant does not appear because $g \cdot b = 0$ and the three with Burgers vectors parallel to the plane of the foil are not observed probably because the internal stress field favors the formation of loops with one of the three inclined Burgers vectors.

Referring to the Thomson tetrahedron Fig. 3, loops lying on the plane opposite apex A are marked α , those opposite apex B, β . The inclination of the planes associated with each loop type is shown in Fig. 4.

The position of the image with respect to the true position is given by the sign of $(g \cdot b)s$. This is "outside" true position for loops marked α and "inside" true position for loops marked β for the bright-field s positive case (Figs. 5a & 5b). Changing g or s causes a change in image position. Table I shows the experimentally observed image positions.

Table I.

	α variant	β variant
Dark field $-g$ s negative, Fig. 1	outside	inside
Dark field $-g$, s positive, Fig. 2	inside	outside
Bright field $+g$ s positive Figs. 5a _ 5b	outside	inside

For images in the s-positive condition a clockwise rotation of the lattice planes causes them to diffract strongly. This is shown in Fig. 3.

In Fig. 4 the lattice plane rotations around interstitial dislocation loops are examined. For the given plane inclinations, experimentally observed contrast is consistent only with interstitial type loops.

ROTATION EXPERIMENTS

Plane inclinations were also determined by large angle (12°) rotation experiments. Figures 5a and b constitute the resulting stereo pair. The foil is rotated about the $[1\bar{1}0]$ the operating reflection (BA, in Fig. 6) as axis. The electron beam is parallel in Fig. 5a to the $[112]$ direction and in Fig. 5b to the $[111]$ direction.

The results of the Kikuchi and stereographic analysis are shown in Figs. 6a and 6b. The arrangement of the tetrahedron of (111) planes for the two orientations are also drawn.

The direction along which defects lie can now be determined by comparing the rotated tetrahedra Figs. 6a and 6b to the bright field micrographs, Figs. 5a and 5b.

The rod CB, for example, must lie along $[\bar{1}01]$. This is side CB of the tetrahedron as drawn in Fig. 6a. The inclined rod marked X changes its position drastically with respect to the rod CB which lies in the foil plane. The rod X therefore lies along DA $[101]$. The end marked X then lies near the top of the foil. (This was directly determined by the dark-field s-negative micrograph, Fig. 1.) Defects lying along CD $[110]$ must foreshorten in length going from the $\langle 112 \rangle$ to the $\langle 111 \rangle$ zone axis. Defects marked B show this behavior.

Therefore the plane inclinations determined by contrast analysis are confirmed.

CONCLUSION

It is shown that the Bell and Thomas dark-field method rapidly provides plane orientations. This together with the imaging conditions can be used to distinguish between interstitial type and vacancy type dislocation loops. The method is used here to determine the nature of small (500Å) loops showing double arc images in silicon. These loops form during the annealing of damage caused by phosphorous-ion implantation. They are shown to be predominantly interstitial in agreement with the conclusion of previous investigations.

The advantage of this method over the more involved rotation and stereographic analysis method recommended by Maher and Eyre⁷ is that only two dark-field micrographs at non-Bragg positions are required. No Kikuchi orientation determination is necessary. Further, the method may be used in microscopes that are not fitted with a high angle goniometer tilt-stage, or for the case of small defects lying in orientations such that large angle rotation does not change their projected area significantly.

ACKNOWLEDGMENTS

We wish to acknowledge the continued support of the U. S. Atomic Energy Commission through the auspices of the Inorganic Materials Research Division of the Lawrence Berkeley Laboratory. We thank Dr. Marcel Bouchard and Mr. T. Astrup for useful discussions. We are grateful to Dr. V. G. K. Reddi of Fairchild R and D, Inc. for helpful comments and the implantation and supply of samples for electron microscopy.

REFERENCES

1. W. L. Bell and G. Thomas, Phil. Mag. 13, 395 (1966).
2. G. Thomas and W. L. Bell, Physica Status Solidi 12, 843 (1965).
3. G. Thomas, Lattice Defects and Their Interactions, R. Hasiguti, ed., (New York, Gordon Breach, 1967) p. 477.
4. M. Wilkins, Modern Diffracting and Imaging Techniques in Materials Science, S. Amelinckx, et al., (Amsterdam, North Holland Publ. 1970), p. 233.
5. S. M. Davidson and G. R. Booker, Rad., Eff. 6, 83 (1970).
6. K. Seshan and J. Washburn, Rad. Eff. 14, 267 (1972).
7. D. M. Maher and B. L. Eyre, Phil. Mag. 23, 409 (1971).

FIGURE CAPTIONS

- Fig. 1 Dark-field (-g) s-negative. The α variant show outside contrast. For this condition, defects near the top surface of the foil are in good contrast. In agreement with stereoanalysis, the top of the rod marked X is seen in good contrast.
- Fig. 2 Dark-field (-g) s-positive. The β variant shows outside contrast. Further, the bottom of the rod, away from X now appears in good oscillating contrast.
- Fig. 3 The two variants α and β are marked adjacent to the planes on which they lie. It is shown that for the s-positive condition a clockwise rotation of the lattice planes will bring them into a strongly diffracting condition.
- Fig. 4 Analysis of loop nature. The lattice plane distortions around defects are examined. The only defects that give images consistent with Table I are interstitial loops.
- Fig. 5a Bright field s-positive near $\langle 112 \rangle$ zone axis. The α variant shows outside and β inside contrast. The rod marked X makes an obtuse angle with rod BC.
- Fig. 5b Same area near $\langle 111 \rangle$ zone axis. The rod X has moved drastically with respect to BC. Note that the defects marked B are smaller than they are in Fig. 5a.
- Fig. 6a & 6b Stereograms and Thomson tetrahedra showing the arrangement of the (111) plane resulting from Kikuchi analysis. Notice that for the rod X to move as it does it must lie

along DA [101]. Then X must denote the top of the rod. Also defects along CD (marked B) must decrease in length going from the $\langle 112 \rangle$ zone axis. Fig. 5a, to the $\langle 111 \rangle$ zone axis, Fig. 5b. Defects marked B show this behavior.



XBB 727-3562

Fig. 2

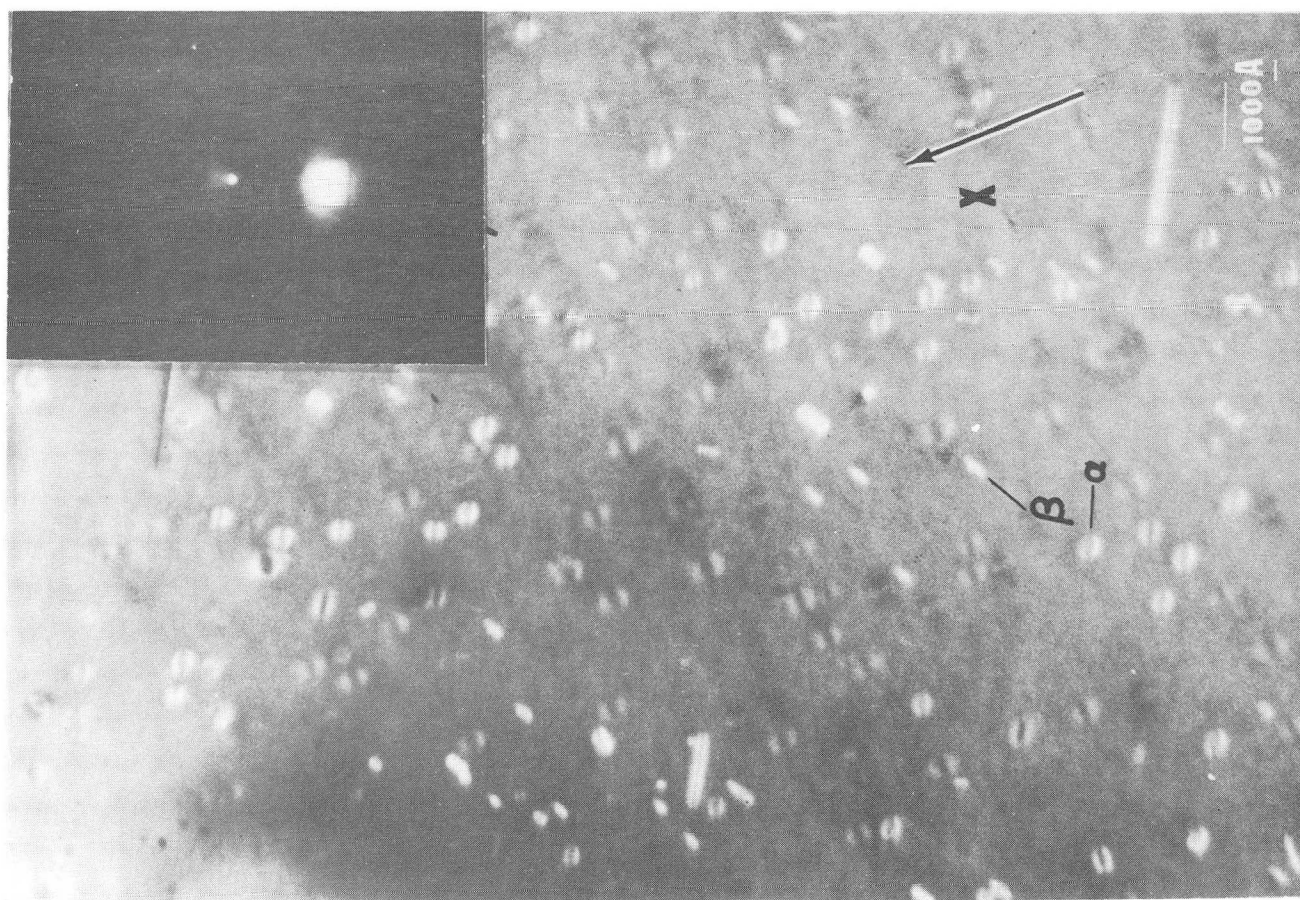


Fig. 1

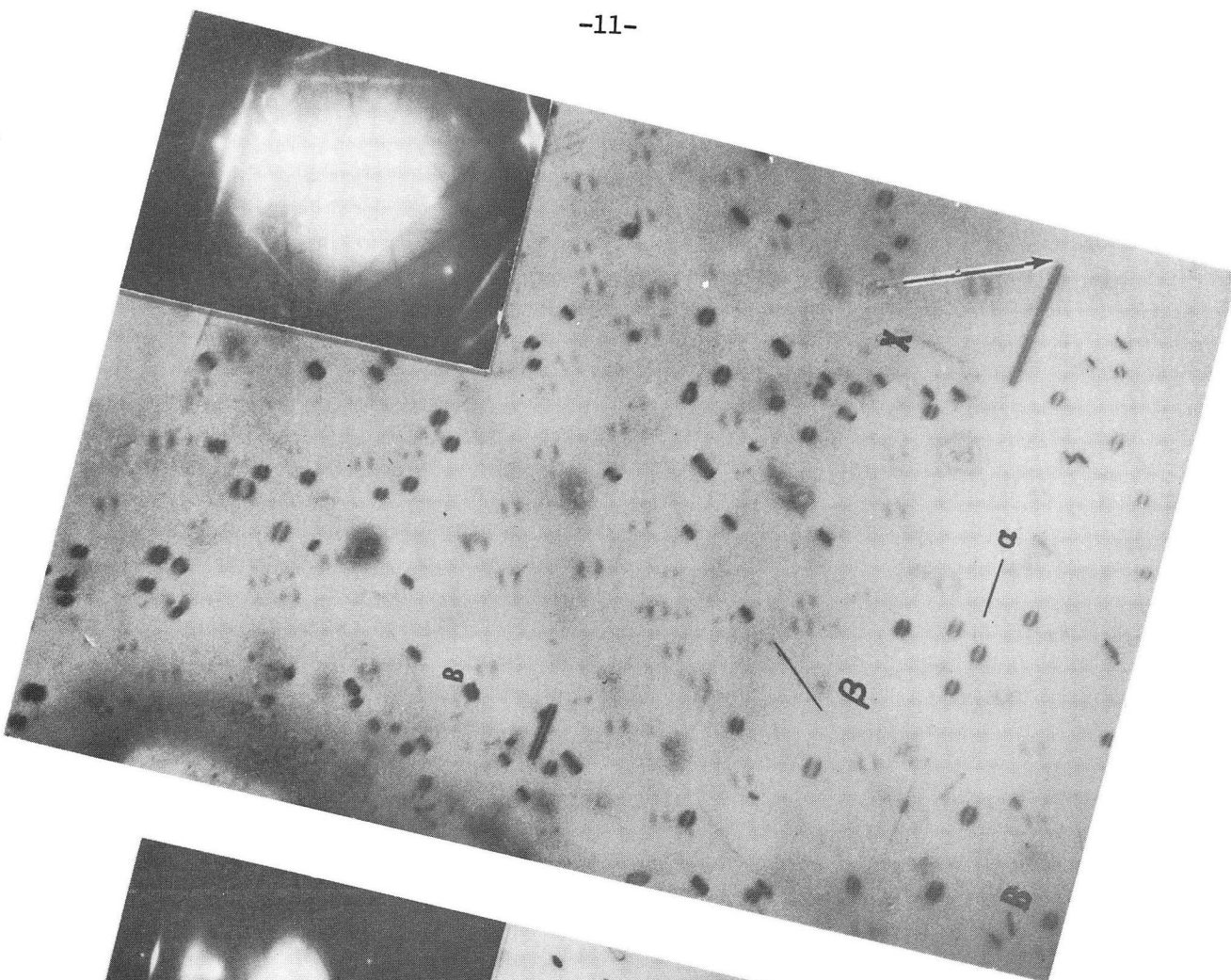


Fig. 5b

XBB 727-3563

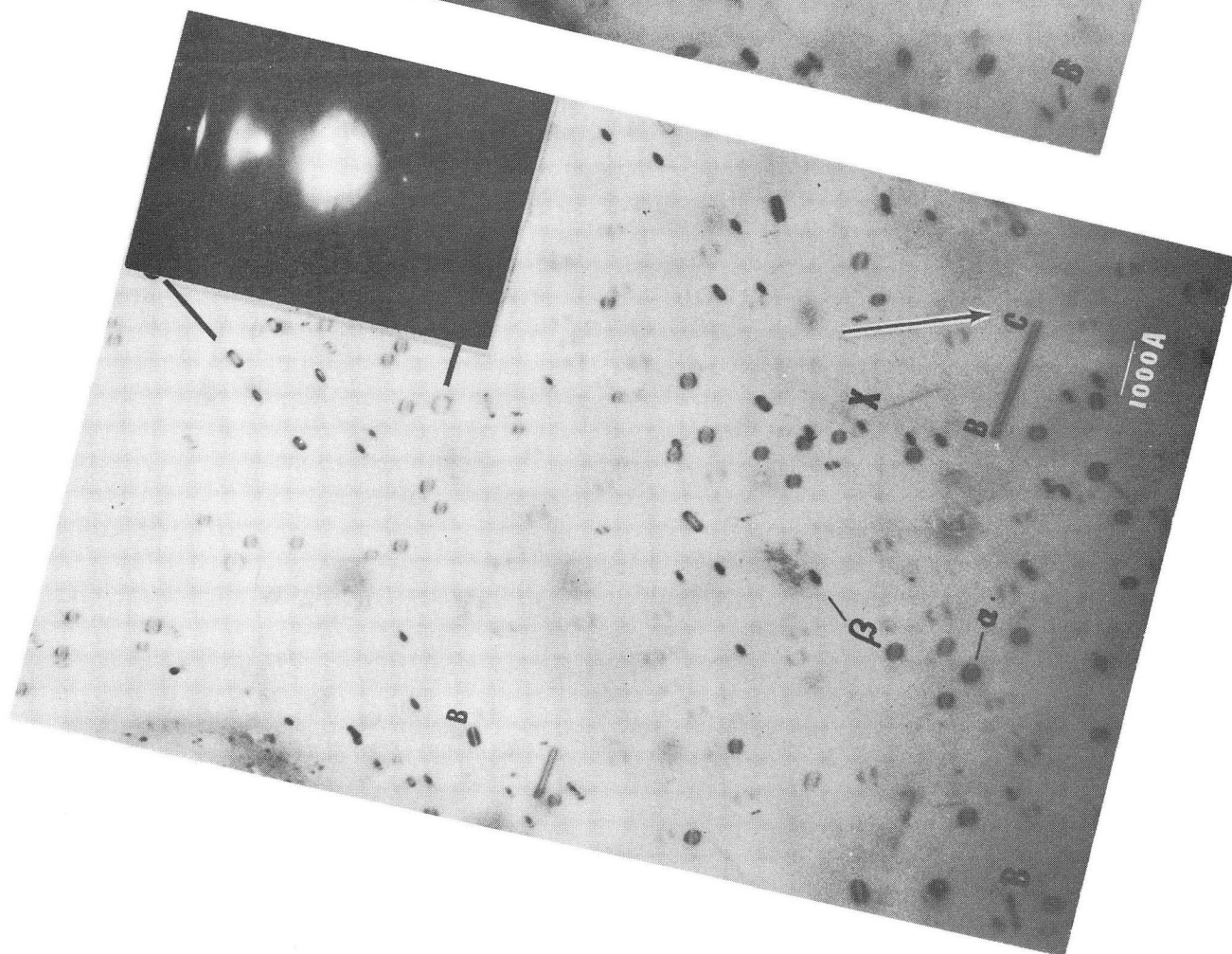


Fig. 5a

LEGAL NOTICE

This report was prepared as an account of work sponsored by the United States Government. Neither the United States nor the United States Atomic Energy Commission, nor any of their employees, nor any of their contractors, subcontractors, or their employees, makes any warranty, express or implied, or assumes any legal liability or responsibility for the accuracy, completeness or usefulness of any information, apparatus, product or process disclosed, or represents that its use would not infringe privately owned rights.

TECHNICAL INFORMATION DIVISION
LAWRENCE BERKELEY LABORATORY
UNIVERSITY OF CALIFORNIA
BERKELEY, CALIFORNIA 94720